Cancer Imaging (2013) **13(4),** 580–590
DOI: 10.1102/1470-7330.2013.0051

REVIEW

Three-dimensional volume-rendered multidetector CT imaging of the posterior inferior pancreaticoduodenal artery: its anatomy and role in diagnosing extrapancreatic perineural invasion

Bhavik N. Patel[a], Craig Giacomini[b], R. Brooke Jeffrey[c], Juergen K. Willmann[c], Eric Olcott[b,d]

[a]Department of Radiology, Duke University Medical Center, Durham, NC, USA; [b]Stanford University School of Medicine, Stanford, CA, USA; [c]Department of Radiology, Stanford Hospital and Clinics, Stanford, CA, USA; [d]Veterans Affairs Health Care System, Palo Alto, CA, USA

Corresponding address: Bhavik N. Patel, Division of Abdominal Imaging, Department of Radiology, Duke University Medical Center, DUMC 3808, Durham, NC 27710, USA.
Email: bhavik.patel@dm.duke.edu

Date accepted for publication 5 November 2013

Abstract

Extrapancreatic perineural spread in pancreatic adenocarcinoma contributes to poor outcomes, as it is known to be a major contributor to positive surgical margins and disease recurrence. However, current staging classifications have not yet taken extrapancreatic perineural spread into account. Four pathways of extrapancreatic perineural spread have been described that conveniently follow small defined arterial pathways. Small field of view three-dimensional (3D) volume-rendered multidetector computed tomography (MDCT) images allow visualization of small peripancreatic vessels and thus perineural invasion that may be associated with them. One such vessel, the posterior inferior pancreaticoduodenal artery (PIPDA), serves as a surrogate for extrapancreatic perineural spread by pancreatic adenocarcinoma arising in the uncinate process. This pictorial review presents the normal and variant anatomy of the PIPDA with 3D volume-rendered MDCT imaging, and emphasizes its role as a vascular landmark for the diagnosis of extrapancreatic perineural invasion from uncinate adenocarcinomas. Familiarity with the anatomy of PIPDA will allow accurate detection of extrapancreatic perineural spread by pancreatic adenocarcinoma involving the uncinate process, and may potentially have important staging implications as neoadjuvant therapy improves.

Keywords: *Pancreatic adenocarcinoma; perineural invasion; posterior inferior pancreaticoduodenal artery.*

Introduction

The pancreas is richly innervated by nerve fibers of the autonomic nervous system extending from the celiac and mesenteric ganglia[1,2]. Retrograde spread of ductal adenocarcinoma along the perineural space of these nerve fascicles is a highly characteristic mode of extrapancreatic dissemination of tumor (Fig. 1)[1,3,4]. Perineural spread of tumor has been implicated as a major factor in the poor prognosis associated with ductal adenocarcinoma of the pancreas, even when the surgical margins appear to be negative and free of tumor[5,6]. A number of neurotropic factors have been found to play a role in facilitating perineural spread of ductal adenocarcinoma; however, there is no association between the actual size of the tumor and the presence of perineural invasion[1,6–8]. Perineural invasion has been detected even in very small pancreatic lesions, frustrating surgical attempts at cure when the primary pancreatic tumor appears to be at an early stage[1,6].

Well-defined perineural pathways along the nerve fascicles of the autonomic nervous system have been identified with careful pathologic dissection[1,2,6,9]. Carcinomas originating in the head and uncinate process of the pancreas characteristically spread via the plexus pancreaticus capitalis 2 (PPC2). The nerve fascicles in this plexus extend from the superior mesenteric ganglion along the posterior inferior pancreaticoduodenal artery

This paper is available online at http://www.cancerimaging.org. In the event of a change in the URL address, please use the DOI provided to locate the paper.

1470-7330/13/000001 + 11
© 2013 International Cancer Imaging Society

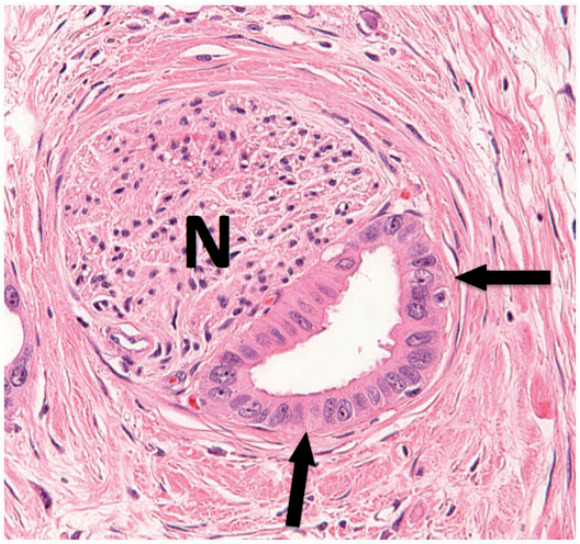

Figure 1 **Histological evidence of perineural invasion in a patient with pancreatic adenocarcinoma. The nerve fascicle (N) in cross section is surrounded by adenocarcinoma cells (arrows) infiltrating the perineural space.**

(PIPDA) to innervate the head and uncinate process of the pancreas[1,6]. Thus, the perineural spread involving PPC2 occurs along the neurovascular bundle of the PIPDA, which therefore serves as an anatomic landmark for detection of perineural spread along this pathway.

Given the poor prognosis of patients with extrapancreatic perineural invasion, preoperative diagnosis with three-dimensional (3D) volume-rendered (VR) multidetector computed tomography (MDCT) could potentially have important staging and treatment implications as neoadjuvant therapy improves. The purpose of this article is to review the MDCT anatomy and anatomic variants of the PIPDA with 3D VR imaging and to emphasize its role in detecting perineural spread along PPC2.

Vascular anatomy

Posterior inferior pancreaticoduodenal artery

The pancreatic head is supplied by branches of the gastroduodenal artery and the superior mesenteric artery (SMA). The gastroduodenal artery gives rise to the superior pancreaticoduodenal artery (SPDA) and the SMA gives rise to the inferior pancreaticoduodenal artery (IPDA). Moreover, the SPDA and IPDA usually give off anterior and posterior branches that form a collateral network with each other (Fig. 2)[10].

The IPDA is the first branch of the SMA, arising approximately 2–5 cm below the takeoff of the SMA from the aorta[10]. The IPDA typically branches into an anterior (AIPDA) and posterior branch (PIPDA) along the posterior medial margin of the pancreas (Fig. 3)[11,12]. The IPDA can be identified in up to 84% of thin-section arterial-phase computed tomography (CT) imaging, and 86% of the time using 3D MDCT[11,12]. In patients with celiac stenosis, there can be retrograde collateral filling of the common hepatic artery from hypertrophied IPDA and gastroduodenal artery (GDA) branches (Fig. 4)[13]. In these cases, the increased flow may result in IPDA aneurysms[14].

There are multiple anatomic variants of the location of the IPDA, including numerous sites of origin from the SMA (Fig. 5)[10]. In addition, there is often considerable anatomic variation of the branching pattern of the IPDA (Table 1). Most commonly, the IPDA originates as a single common trunk from the SMA leading to both AIPDA and PIPDA (Figs. 2A and 6).

However, the IPDA may arise from the first jejunal branch rather than from the SMA (Fig. 7)[10,11]. This is the most common anatomic variant of the IPDA, and is sometimes referred to as the pancreaticoduodenal-jejunal trunk (PDJ trunk)[10]. A less common anatomic variant is an origin of the IPDA from a replaced right hepatic artery off the SMA, or sharing a common origin with a second-order jejunal branch or the dorsal pancreatic artery (Fig. 8)[10,11]. Branching variations include separate origins of the AIPDA and PIPDA arising directly off the SMA or the first-order jejunal branch[11]. Finally, the pancreaticoduodenal arcade may also develop as a single arterial channel rather than a network of anastomoses between anterior and posterior branches of the SPDA and IPDA (Fig. 5)[13].

Extrapancreatic neural plexus

The head of the pancreas is innervated by neural fibers extending from the celiac and mesenteric ganglia[1,2]. Four extrapancreatic pathways of perineural spread have been described (Fig. 9, Table 2)[1,2,9]. Plexus pancreaticus capitalis 1 (PPC1) extends from the right celiac ganglion to the upper medial uncinate margin via a course posterior to the portal vein. Plexus pancreaticus capitalis 2 (PPC2) consists of nerve fibers extending from the mesenteric plexus to the uncinate process along the course of the PIPDA[1,2,6,15]. Thus, retrograde extension of tumor from carcinomas of the caudal margin of the head of the pancreas and uncinate process frequently extends along the PPC2 pathway to ultimately involve the mesenteric ganglion and result in SMA encasement[1,16]. Adenocarcinomas in the more cranial head of the pancreas typically extend along the PPC1 pathway[1].

Certain relative locations of adenocarcinoma within the pancreatic head can be associated with a specific pathway of perineural spread. For example, a tumor arising in the ventral pancreatic head typically spreads toward the SMA plexus, whereas dorsally located pancreatic head tumors tend to spread toward the common

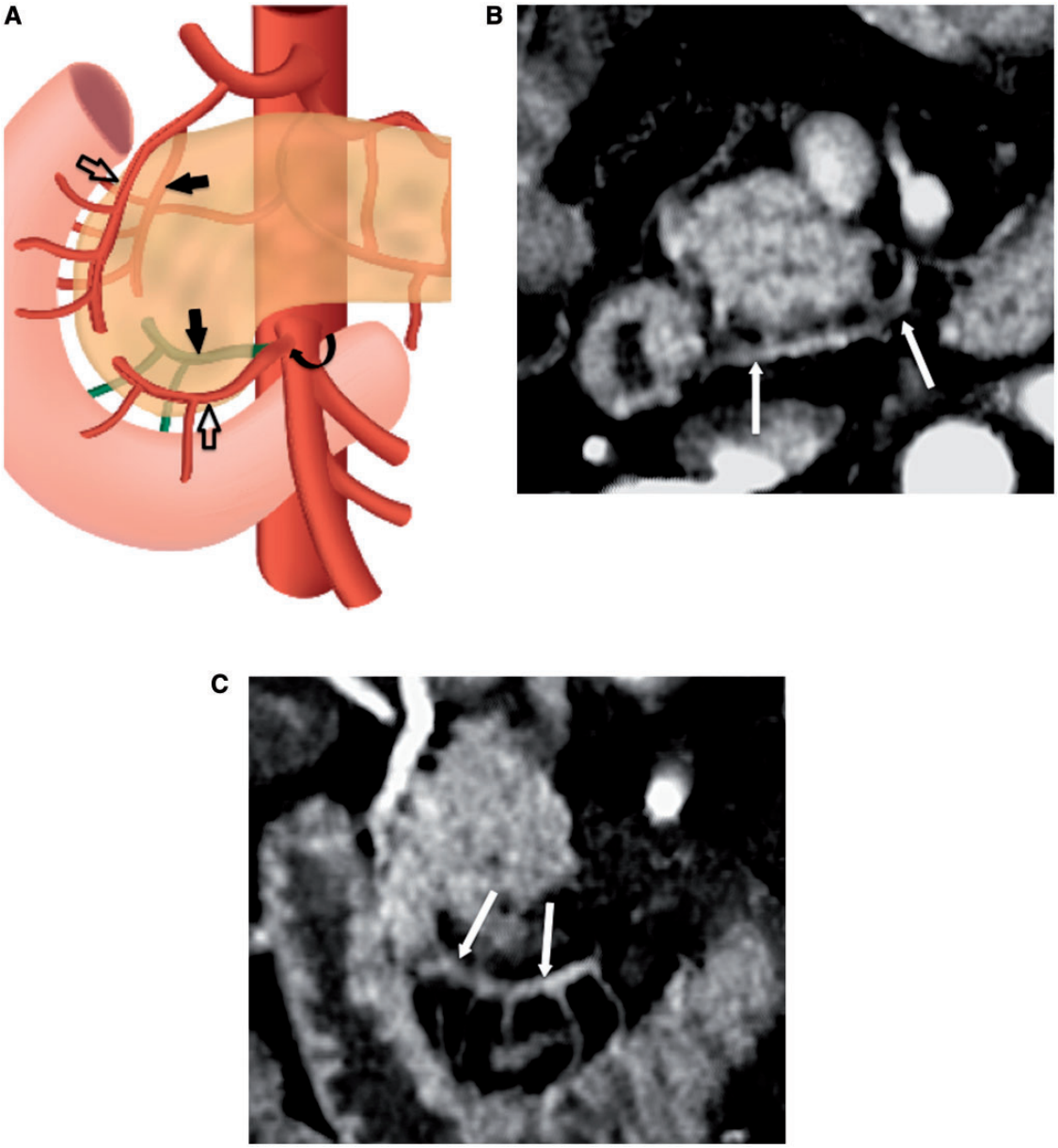

Figure 2 **Schematic (A) shows the normal origin of the posterior inferior pancreaticoduodenal artery (PIPDA) (green) and anterior inferior pancreaticoduodenal artery (AIPDA) arising from the inferior pancreaticoduodenal artery (IPDA) (curved arrow). A normal pancreaticoduodenal arcade is also shown with an anastomotic network between the branches of the superior pancreaticoduodenal artery (SPDA) and IPDA (black arrows). The anterior arcade (open arrows) is formed by the anterior superior pancreaticoduodenal and anterior inferior pancreaticoduodenal arteries. The posterior arcade (solid arrows) is formed by the posterior superior pancreaticoduodenal and posterior inferior pancreaticoduodenal arteries. Axial (B) and coronal (C) three-dimensional (3D) volume-rendered computed tomography (CT) images show the posterior pancreaticoduodenal arcade (arrows).**

hepatic artery and the hepaticoduodenal ligament plexuses[9]. The latter course, whereby tumors of the dorsal pancreatic head spread along the GDA and common hepatic artery, ultimately toward the right celiac ganglion, is known as the anterior pathway[1]. Finally, a relatively less frequent pathway that also involves the PIPDA is the root of mesentery (RoM) pathway of spread. The RoM follows a path similar to that of PPC2 but spreads caudally at the SMA to infiltrate the mesentery, rather than extending toward the celiac ganglion[1].

MDCT observation population

We obtained approval from the institutional review board for retrospective imaging analysis of the patients in this

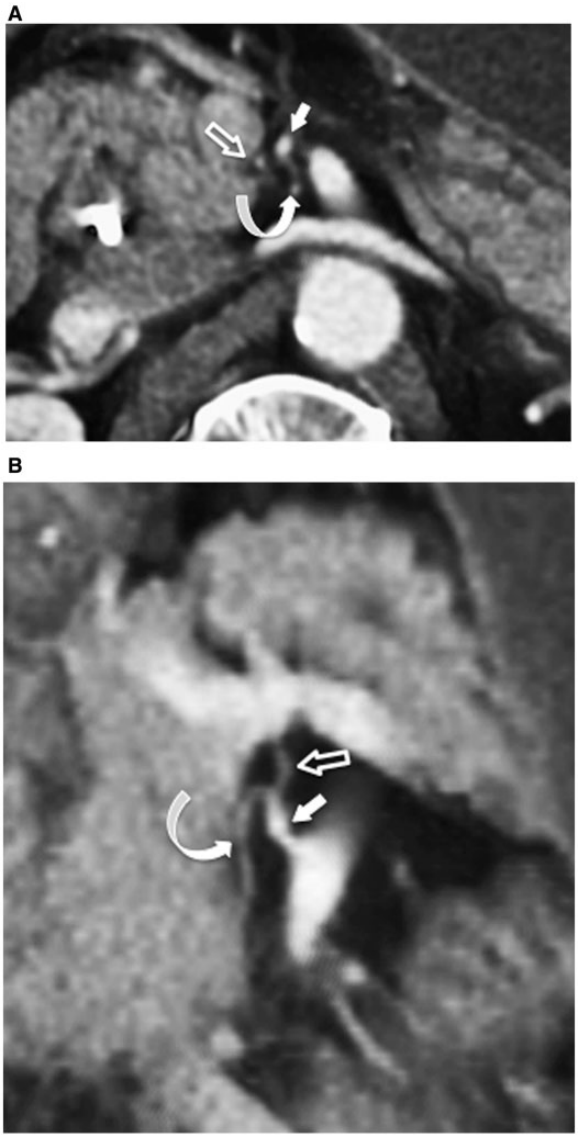

Figure 3 **Normal origin of the IPDA and branching pattern. Axial (B) and coronal (C) 3D volume-rendered multidetector CT (MDCT) images from a 78-year-old man with obstructive jaundice shows the IPDA (solid arrow) originating from the SMA and giving rise to AIPDA (open arrow) and PIPDA (curved arrow).**

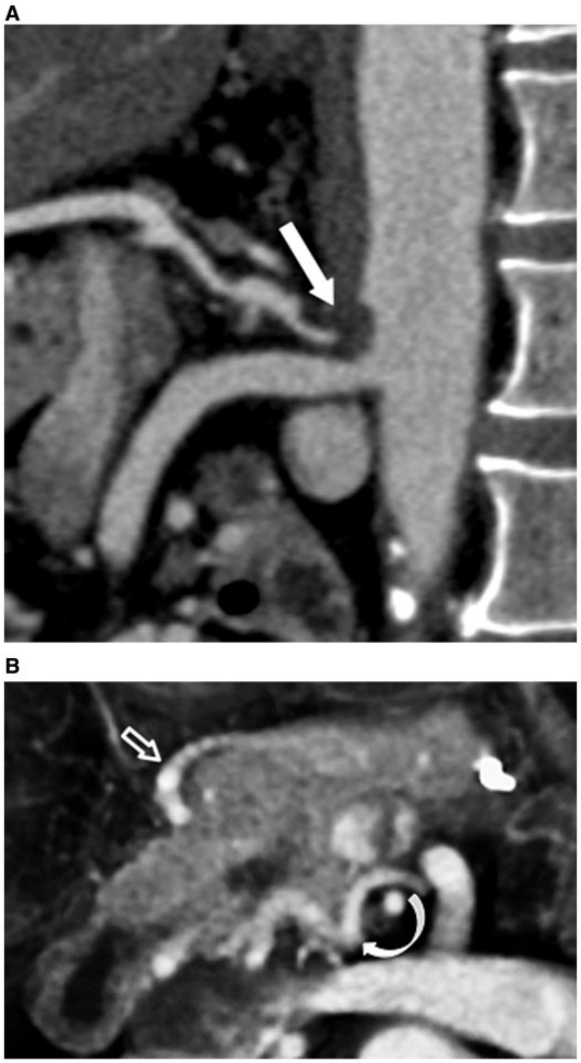

Figure 4 **IPDA prominence in celiac artery stenosis in a 60-year-old man, status post distal pancreatectomy and splenectomy for a pancreatic neuroendocrine tumor. Sagittal (A) arterial-phase CT image shows a significant celiac axis stenosis (arrow). Axial 3D volume-rendered image (B) shows the PIPDA (curved arrow) and the AIPDA (short arrow).**

series. We analyzed the MDCT findings of 184 adult patients who underwent evaluation for a possible pancreatic mass. After careful review of the 3D VR images, the anatomy of the IPDA was delineated and classified into one of the following categories: SMA origin, common origin with the first jejunal branch, or indeterminate. We also determined the branching pattern of the IPDA and the origin of the PIPDA. Of the 84 adult males and 100 adult females, we found 94 (51%) of the patients had the IPDA originating as the first branch off the SMA, and 61 (33%) had the IPDA originating from a common trunk with the first jejunal branch (PDJ trunk). All 155 patients showed a normal branching pattern of the IPDA into the AIPDA and PIPDA with a normal course. The anatomy was difficult to clearly delineate in 29 (15%) of the patients, most commonly because of a lack of complete visualization of these small-caliber vessels. The results of this analysis are summarized in Table 3. Although our observations are within the range of the incidence reported for the various anatomical patterns, there is wide variation in the literature. For example, the origin of the IPDA from SMA has been reported to be seen in 5–100% of patients, and the PDJ trunk has been reported to be seen in 20–65% of cases[10].

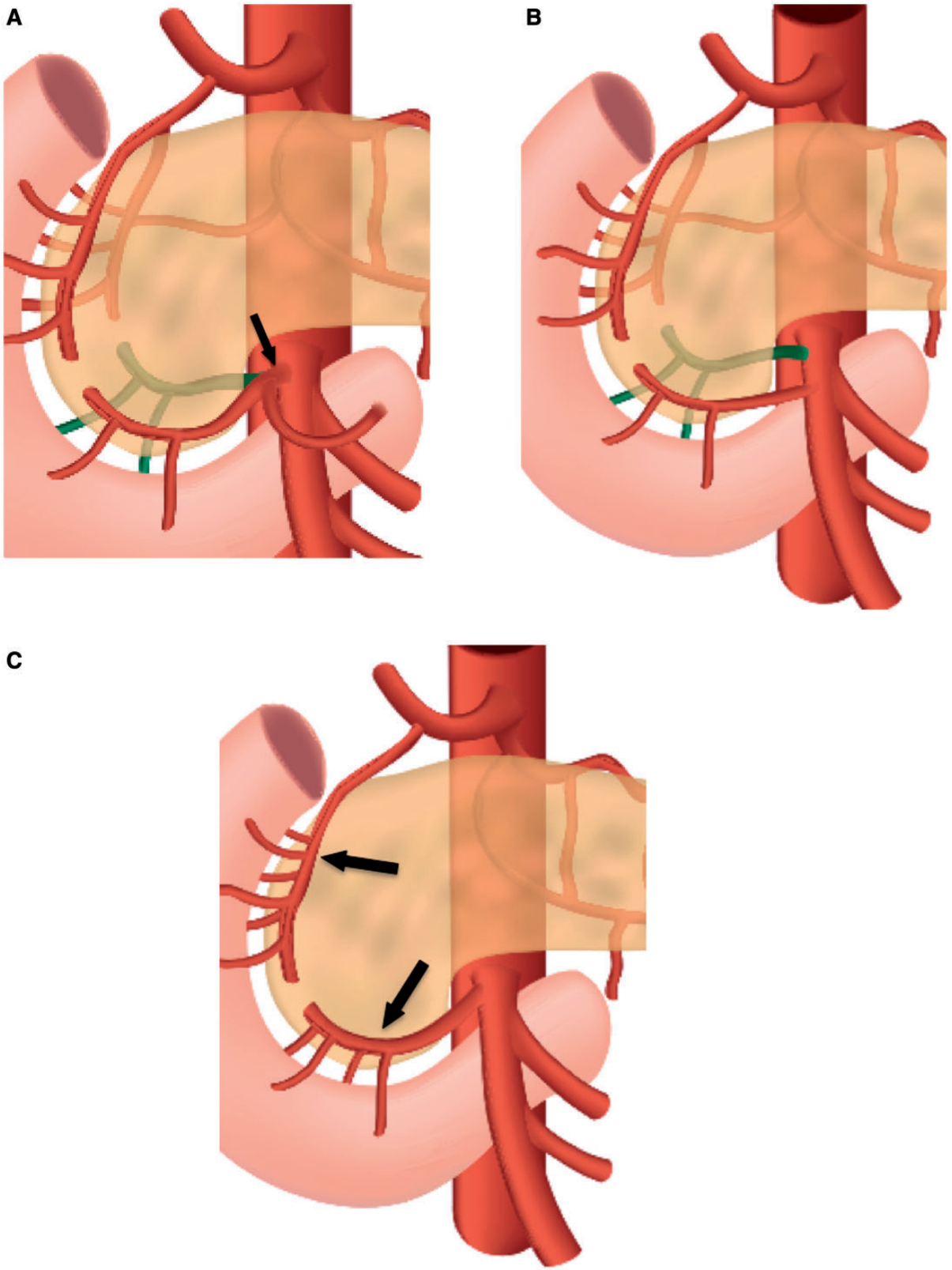

Figure 5 **Variations in origin of IPDA. Coronal schematics show variations in the PIPDA (shown in green) origin, including origination from the common pancreaticoduodenal-jejunal trunk (A), separate origins of the AIPDA and PIPDA (B), and single pancreaticoduodenal arcade (C, arrows).**

Table 1 **Summary of variations in the origin and branching pattern of the IPDA**

Variations in IPDA origin[10,11]	Variations in IPDA branching[11,13]
Common IPDA originating from SMA	Common IPDA gives rise to AIPDA and PIPDA
IPDA originating with first jejunal branch as a common trunk (PDJ)	Separate origin of the AIPDA and PIPDA from first jejunal branch
Common IPDA originating off the replaced right hepatic artery	Separate origin of the AIPDA and PIPDA from SMA
IPDA originating with the second jejunal branch as a common trunk	Separate origin of the AIPDA and PIPDA, one from first jejunal branch and the other from the SMA
IPDA originating with the dorsal pancreatic artery as a common trunk	Single-channel IPDA (no division into AIPDA and PIPDA)
Common IPDA originating from a common trunk involving the first 2–3 jejunal branches[a]	
Common IPDA originating from middle colic artery[a]	

IPDA, inferior pancreaticoduodenal artery; AIPDA, anterior inferior pancreaticoduodenal artery; PIPDA, posterior inferior pancreaticoduodenal artery; PDJ, pancreaticoduodenal-jejunal; SMA, superior mesenteric artery.
[a]Rare.

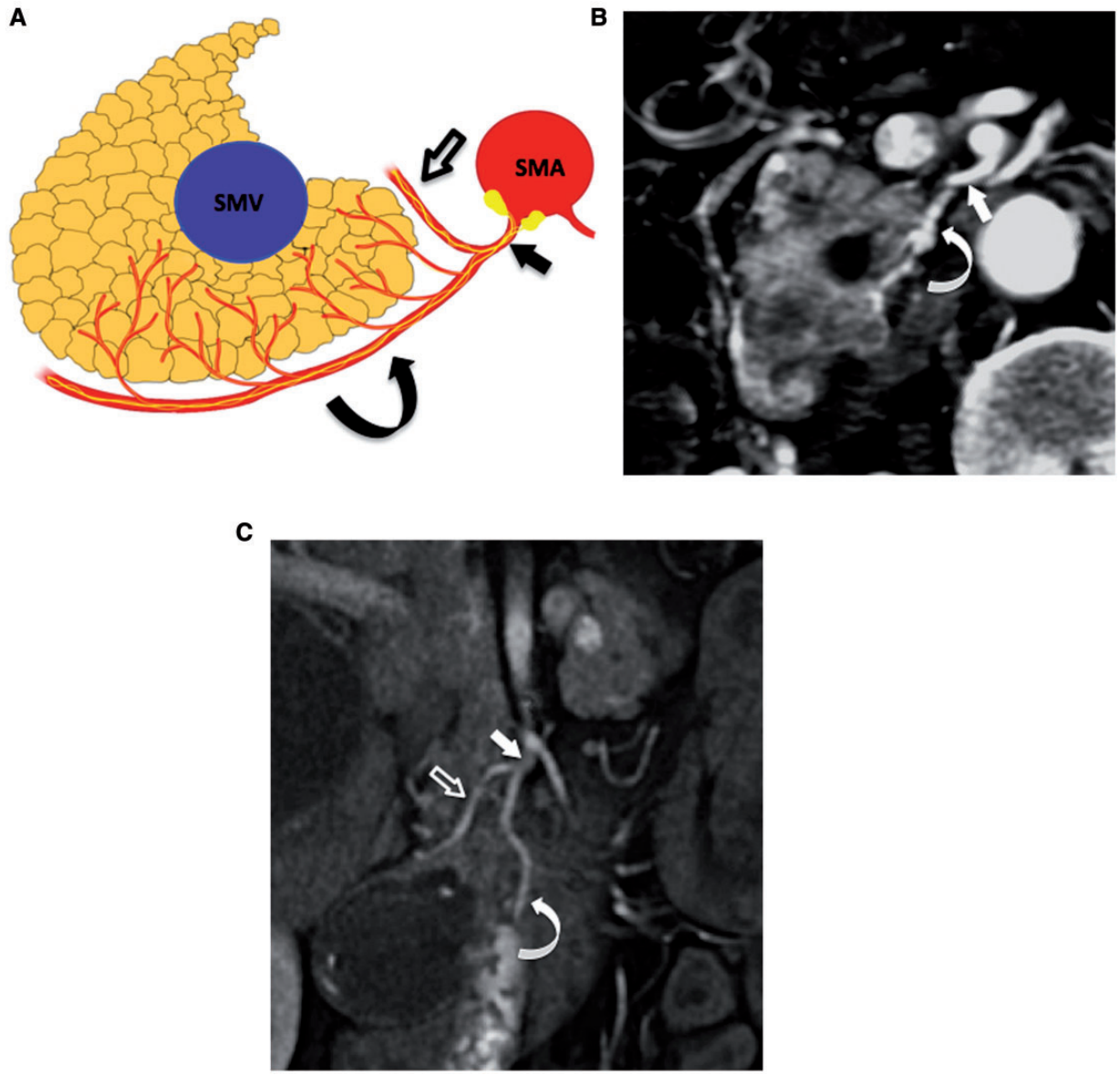

Figure 6 **Normal PIPDA anatomy. Axial schematic (A), axial 3D volume-rendered image (B), and coronal 3D volume-rendered image (C) show the PIPDA (curved arrow) and AIPDA (open arrow) originating off the IPDA (solid arrow). SMA, superior mesenteric artery; SMV, superior mesenteric vein.**

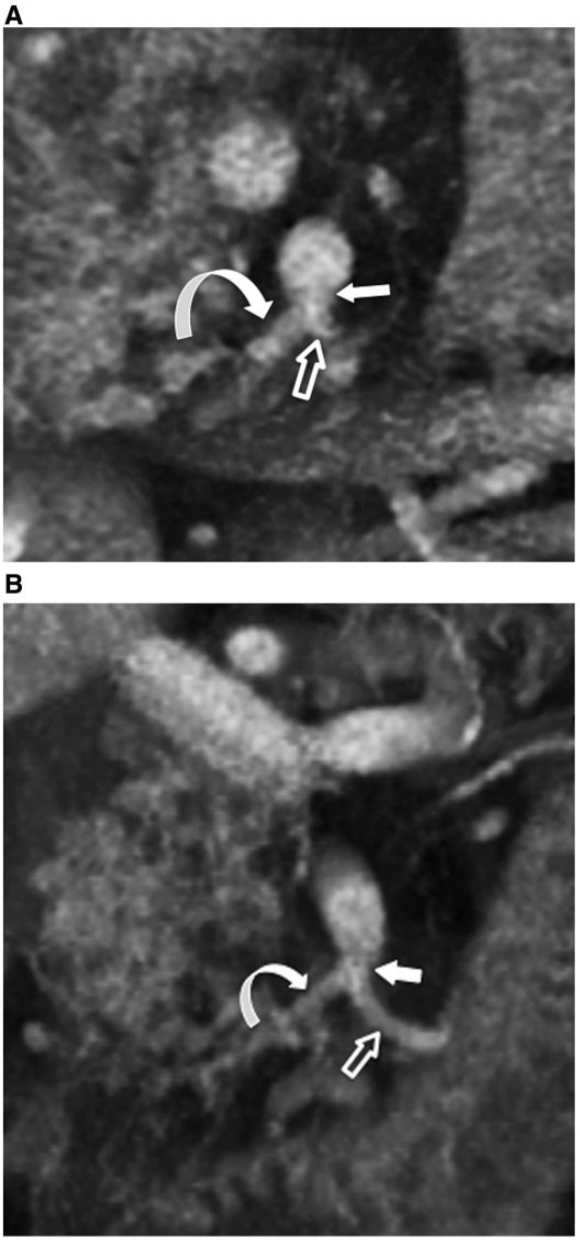

Figure 7 **Origin of the IPDA as a common trunk with the first jejunal branch. Axial (A) and coronal (B) 3D volume-rendered MDCT images show a common trunk (solid arrow) giving rise to the IPDA (curved arrow) and the first jejunal branch (open arrow).**

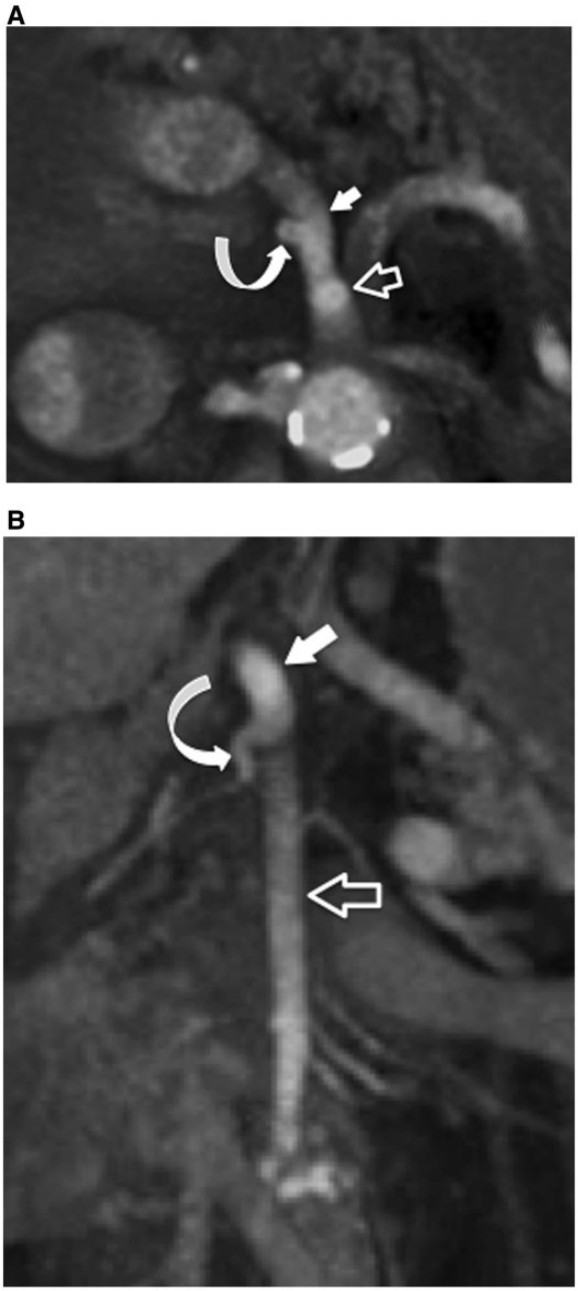

Figure 8 **Variation in the origin of the IPDA in a 59-year-old woman undergoing workup for a pancreatic mass. Axial (A) and coronal (B) 3D volume-rendered MDCT images show a replaced right hepatic artery (solid arrow) off the SMA (open arrow) that gives rise to the IPDA (curved arrow).**

MDCT diagnosis of perineural invasion

MDCT technique

The details of the pancreatic protocol CT and postprocessing techniques have been described previously[1,17]. Images were obtained on either a LightSpeed 16-row MDCT (GE Healthcare) or a Somatom Sensation 64-row MDCT (Siemens Medical Solutions) scanner. Immediately prior to scanning, patients were asked to drink approximately 500–700 ml of a water-based neutral contrast (VoLumen, EZ-EM) to distend the duodenum. A nonionic contrast agent (150 ml) was injected at 4 ml/s. A biphasic breath-hold examination was performed, with a late arterial-phase image acquired at 35–40 s and portal venous-phase image at 60–70 s. Images were acquired at 0.625-mm or 1.25-mm slice thickness.

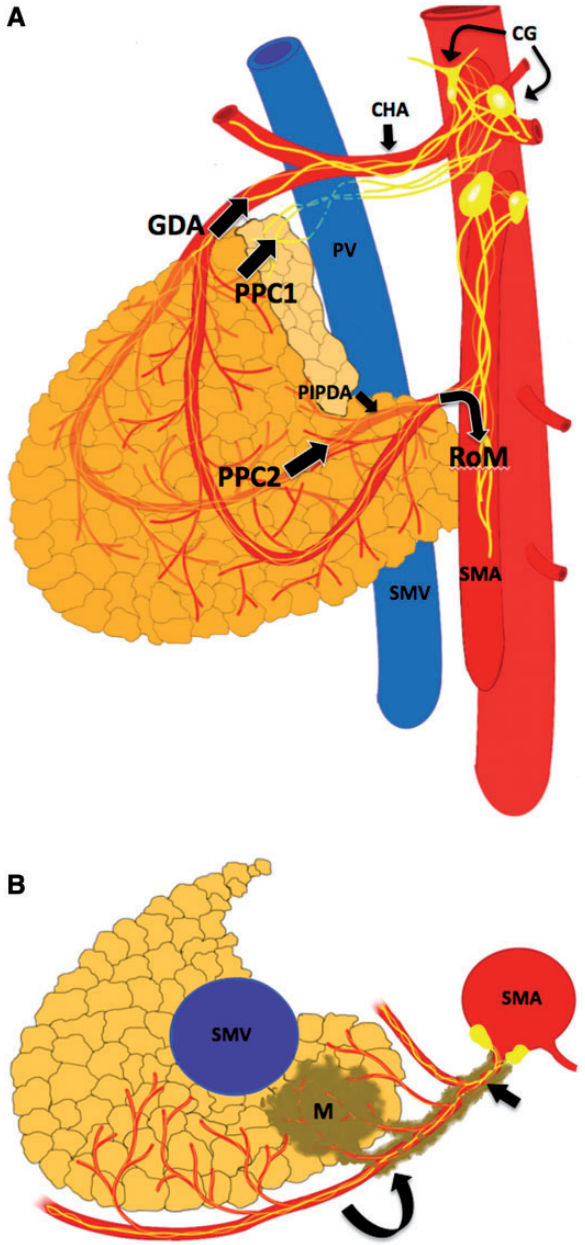

Figure 9 **Four pathways of extrapancreatic perineural spread. Coronal schematic (A) shows the 4 pathways of extrapancreatic perineural spread. Plexus pancreaticus capitalis 1 (PPC1) extends posterior to the portal vein (PV) from the pancreatic head to the celiac ganglion (CG). Plexus pancreaticus capitalis 2 (PPC2) spreads along the posterior inferior pancreaticoduodenal artery (PIPDA) toward the mesenteric ganglion. Root of mesentery (RoM) involves spread along the PIPDA but extends caudally along the superior mesenteric artery (SMA) to the mesenteric root. The anterior or gastroduodenal artery (GDA) pathway extends along the GDA and common hepatic artery (CHA), ultimately toward the CG. Axial schematic (B) shows an uncinate mass (M) with perineural spread along the PIPDA (curved arrow) and IPDA (solid arrow) toward the SMA, typical of the PPC2 pathway. SMV, superior mesenteric vein.**

Table 2 **Four pathways of extrapancreatic perineural spread**

Pathways of perineural spread[1,2,9]
Plexus pancreaticus capitalis 1
Plexus pancreaticus capitalis 2
Gastroduodenal artery to common hepatic artery plexus (anterior pathway)
Root of mesentery

Table 3 **Observed IPDA origin and branching anatomy**

Anatomy	No. (%) of patients ($N = 184$)
IPDA origin off SMA	94 (51)
Common IPDA and first jejunal branch trunk	61 (33)
Indeterminate anatomy	29 (16)
Normal branching of IPDA into PIPDA and AIPDA	155

Volumetric postprocessing

After image acquisition, image processing was performed on dedicated 3D workstations (Volume Viewer; GE Healthcare) by specially trained imaging technologists. On axial CT data sets, volumetric slabs were generated in a 20° right coronal oblique plane. This obliquity allows optimal visualization of the duodenal sweep and to stay parallel with the common bile duct. The studies were reformatted along this plane using a small (12 cm) field of view. A second small-field-of-view volumetric slab was also generated in a plane perpendicular to the SMA to optimize visualization of the mesenteric neural plexus. 3D images were generated at 1-mm intervals with the volume anterior to the cut plane visualized on each image. This resulted in a slice thickness of 1 mm in the volumetric slab. Scrollable 3D data sets focused on the region of interest were generated as a result. Images were depicted in gray-scale to detect subtle attenuation differences and preserve familiarity for referring physicians.

Detection of perineural invasion

Perineural invasion is evident on CT when there is direct extension of tumor involving a known perineural pathway. Specifically, perineural invasion appears as confluent soft tissue replacing the fat around peripancreatic vessels with attenuation similar to that of the primary pancreatic lesion[1]. Mochizuki et al.[18] found that the presence of soft tissue attenuating stranding greater than 2 mm was associated with perineural invasion in greater than 90% of patients with pancreatic head carcinomas. This is in contradistinction to lymphatic invasion whereby a reticular or tubular pattern is seen, although

some overlap with perineural invasion is seen, as lymphatic invasion can appear as soft tissue mass-like density[19]. Appearance of perineural invasion on magnetic resonance imaging has also been similarly described as streak-like signal intensity replacing the normal peripancreatic fat[20].

The PIPDA is the anatomic landmark for the neurovascular bundle involving PPC2[1,16]. Perineural invasion along the PIPDA obliterates the fat planes adjacent to this vessel and is seen to directly connect the tumor to the SMA (Figs. 10 and 11)[1,6,16]. Because the PIPDA is a small anatomic structure (1–2 mm), high-resolution small field of view 3D VR imaging during a late arterial-phase acquisition is optimal for depiction of the fat planes along this vessel. Scrolling through the cut-plane VR images allows excellent depiction of the course of the PIPDA along the posterior inferior margin of the uncinate process and pancreatic head. Tumors of the uncinate process typically result in hypodense masses that enlarge the uncinate and cause its contours to extend in a convex margin, giving it a rounded appearance[16].

Current guidelines for the staging of ductal adenocarcinoma do not take into consideration extrapancreatic spread along perineural pathways[21–23]. Nevertheless, increasing awareness of the ability of 3D VR MDCT to diagnose perineural invasion along such clearly defined anatomic pathways may ultimately lead to a reappraisal of these staging guidelines. Reliable preoperative

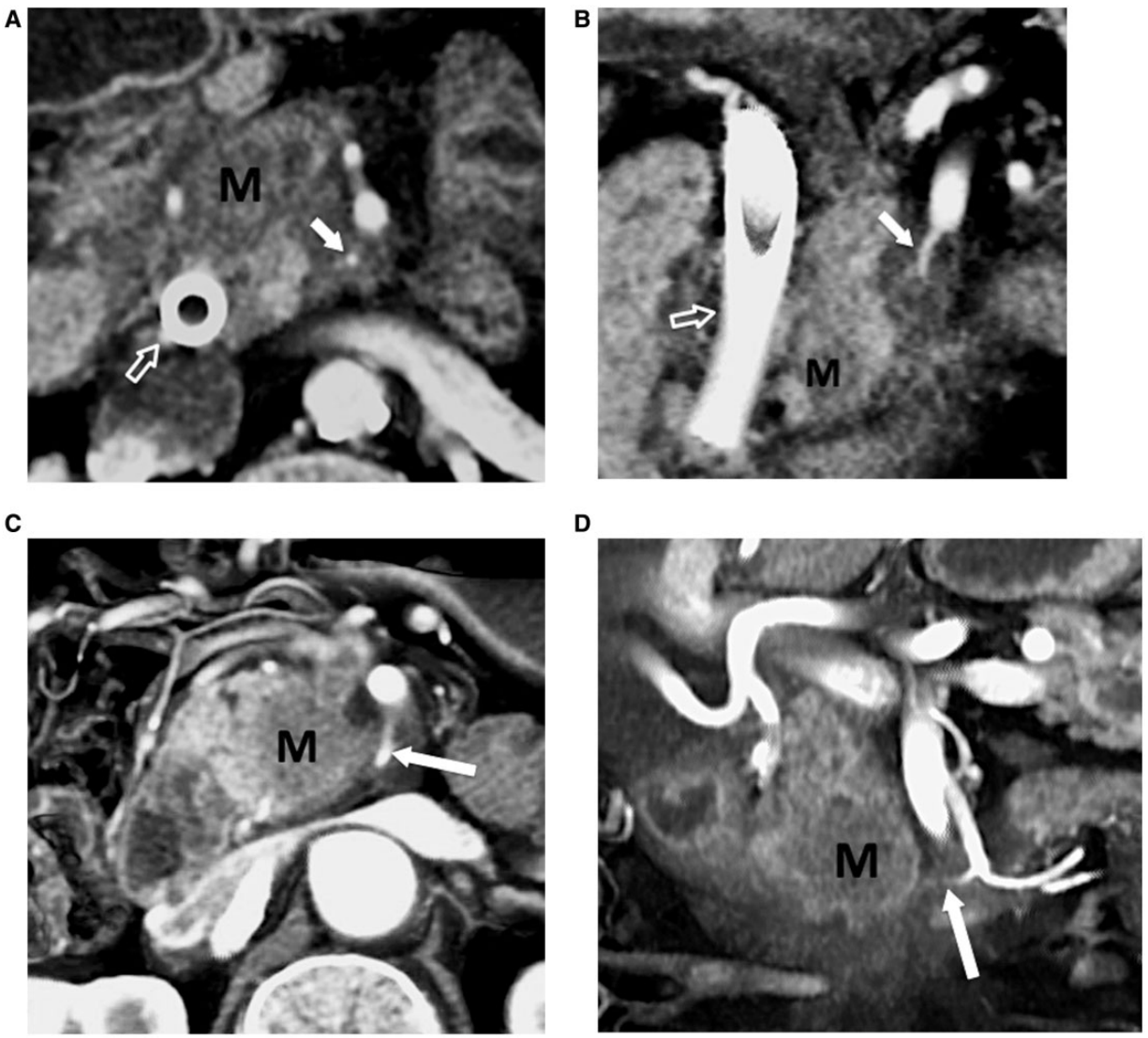

Figure 10 **Extrapancreatic perineural invasion along the PIPDA. Axial (A) and coronal (B) 3D volume-rendered images in a patient with a pancreatic head adenocarcinoma (M) shows perineural invasion along the PIPDA (solid arrow) and a biliary stent in place (open arrow). Additional axial (C) and coronal (D) images from different patients show pancreatic head adenocarcinoma (M) with perineural invasion (arrow) along the PIPDA extending up to the SMA.**

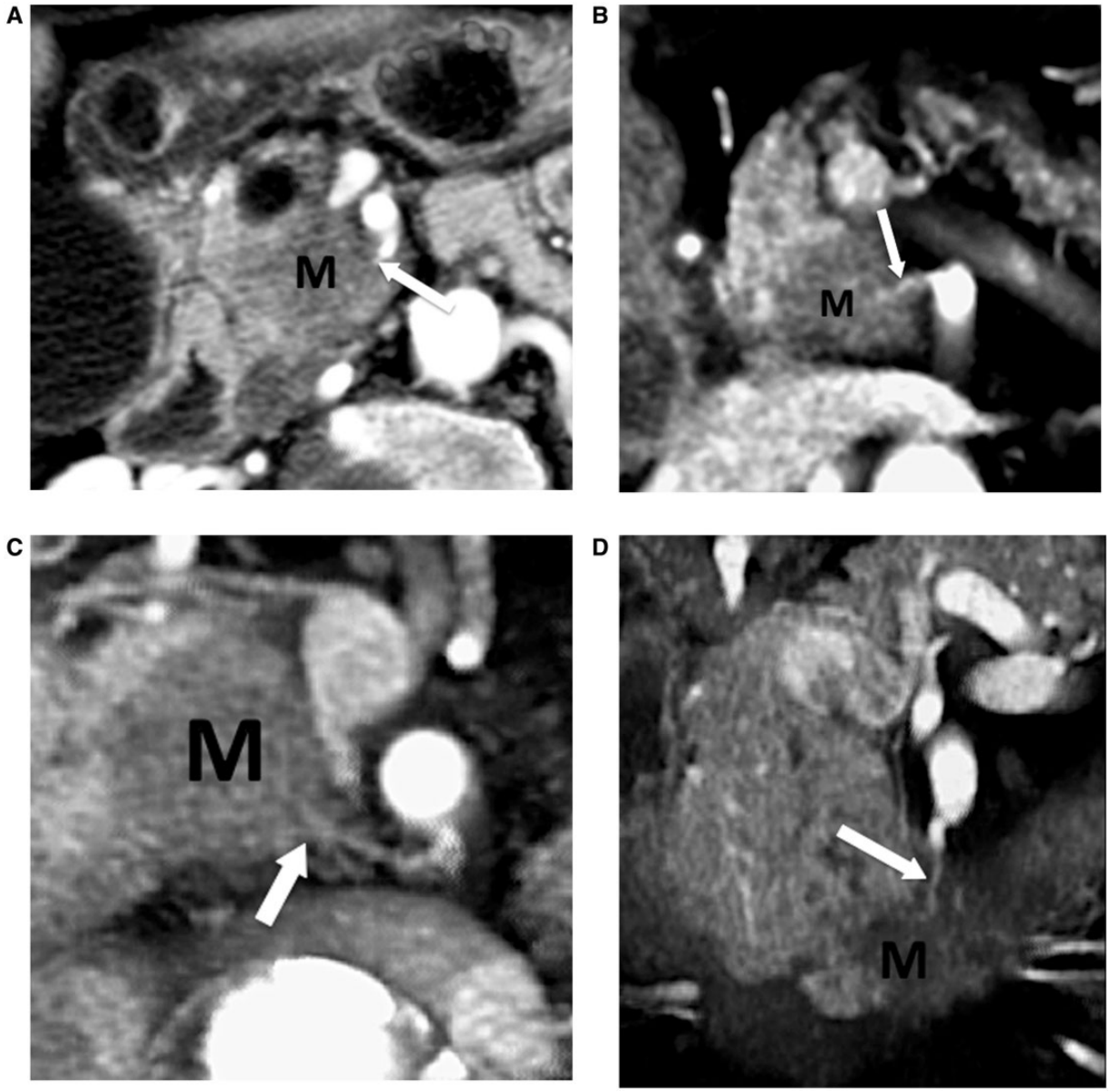

Figure 11 **Extrapancreatic perineural invasion along the PIPDA. Axial (A, B, C) and coronal (D) 3D volume-rendered images in different patients with pancreatic uncinate adenocarcinoma (M) shows perineural invasion along the PIPDA (solid arrow).**

diagnosis of extrapancreatic and perineural invasion of ductal adenocarcinoma might in the future indicate the need for neoadjuvant therapy prior to attempted resection, to reduce the likelihood of positive surgical margins. Although thin-section MDCT and multiplanar reformation has been shown to have an accuracy of 95% in detecting perineural invasion, these techniques were not able to adequately resolve small second-order peripancreatic vessels[6,18]. For example, Tian et al.[6] showed accuracy in detection of perineural invasion using the IPDA as a landmark. 3D VR MDCT is able to resolve smaller second-order vessels, such as the PIPDA, and may therefore allow earlier detection of perineural invasion. However, further studies are needed to validate the overall accuracy of 3D VR MDCT and to compare it with conventional techniques, especially in cases of early perineural invasion.

Conclusion

Perineural invasion from pancreatic adenocarcinoma is a characteristic mode of extrapancreatic spread, and confers a poor prognosis. The pathway of perineural spread for adenocarcinomas involving the uncinate process is typically via the PPC2 pathway, for which the PIPDA

serves as key anatomic landmark. PPC2 perineural invasion can be diagnosed on MDCT when direct tumor extension is identified along the PIPDA, and 3D VR imaging is an ideal method to display this pattern of invasion. Further studies are needed, however, to evaluate the overall accuracy of the 3D VR MDCT diagnosis of perineural spread in patients who have undergone Whipple procedure. While surgical staging classifications for pancreatic adenocarcinoma do not currently include assessment of extrapancreatic perineural spread, this may become more important in the future if neoadjuvant therapy becomes more effective.

Acknowledgements

Medical illustrations were provided by Bhavik Patel and Amy Morris.

Conflict of interest

The authors declare that they have no conflicts of interest.

References

[1] Deshmukh SD, Willmann JK, Jeffrey RB. Pathways of extrapancreatic perineural invasion by pancreatic adenocarcinoma: evaluation with 3D volume-rendered MDCT imaging. AJR Am J Roentgenol 2010; 194: 668–674. doi: 10.2214/AJR.09.3285.

[2] Yoshioka H, Wakabayashi T. Therapeutic neurotomy on head of pancreas for relief of pain due to chronic pancreatitis; a new technical procedure and its results. AMA Arch Surg 1958; 76: 546–554.

[3] Miyazaki I. [Perineural invasion and surgical treatment of the pancreas head cancer]. Nihon Geka Gakkai Zasshi 1997; 98: 646–648.

[4] Verbeke CS. Resection margins and R1 rates in pancreatic cancer–are we there yet? Histopathology 2008; 52: 787–796. doi: 10.1111/j.1365-2559.2007.02935.x.

[5] Nakao A, Harada A, Nonami T, Kaneko T, Takagi H. Clinical significance of carcinoma invasion of the extrapancreatic nerve plexus in pancreatic cancer. Pancreas 1996; 12: 357–361.

[6] Tian H, Mori H, Matsumoto S, et al. Extrapancreatic neural plexus invasion by carcinomas of the pancreatic head region: evaluation using thin-section helical CT. Radiat Med 2007; 25: 141–147. doi: 10.1007/s11604-006-0115-1.

[7] Dang C, Zhang Y, Ma Q, Shimahara Y. Expression of nerve growth factor receptors is correlated with progression and prognosis of human pancreatic cancer. J Gastroenterol Hepatol 2006; 21: 850–858. doi: 10.1111/j.1440-1746.2006.04074.x.

[8] Zhu Z, Friess H, diMola FF, et al. Nerve growth factor expression correlates with perineural invasion and pain in human pancreatic cancer. J Clin Oncol 1999; 17: 2419–2428.

[9] Makino I, Kitagawa H, Ohta T, et al. Nerve plexus invasion in pancreatic cancer: spread patterns on histopathologic and embryological analyses. Pancreas 2008; 37: 358–365.

[10] Bertelli E, Di Gregorio F, Bertelli L, Civeli L, Mosca S. The arterial blood supply of the pancreas: a review. III. The inferior pancreaticoduodenal artery. An anatomical review and a radiological study. Surg Radiol Anat 1996; 18: 67–74.

[11] Sakaguchi T, Suzuki S, Inaba K, Takehara Y, Nasu H, Konno H. Peripancreatic arterial anatomy analyzed by 3-dimensional multidetector-row computed tomography. Hepatogastroenterology 2012; 59: 1986–1989. doi: 10.5754/hge11787.

[12] Chong M, Freeny PC, Schmiedl UP. Pancreatic arterial anatomy: depiction with dual-phase helical CT. Radiology 1998; 208: 537–542.

[13] Song SY, Chung JW, Kwon JW, et al. Collateral pathways in patients with celiac axis stenosis: angiographic-spiral CT correlation. Radiographics 2002; 22: 881–893.

[14] Kallamadi R, Demoya MA, Kalva SP. Inferior pancreaticoduodenal artery aneurysms in association with celiac stenosis/occlusion. Semin Intervent Radiol 2009; 26: 215–223. doi: 10.1055/s-0029-1225671.

[15] Zuo HD, Zhang XM, Li CJ, et al. CT and MR imaging patterns for pancreatic carcinoma invading the extrapancreatic neural plexus (part I): anatomy, imaging of the extrapancreatic nerve. World J Radiol 2012; 4: 36–43. doi: 10.4329/wjr.v4.i2.36.

[16] Padilla-Thornton AE, Willmann JK, Jeffrey RB. Adenocarcinoma of the uncinate process of the pancreas: MDCT patterns of local invasion and clinical features at presentation. Eur Radiol 2012; 22: 1067–1074. doi: 10.1007/s00330-011-2339-4.

[17] Pham DT, Hura SA, Willmann JK, Nino-Murcia M, Jeffrey RB. Jr. Evaluation of periampullary pathology with CT volumetric oblique coronal reformations. AJR Am J Roentgenol 2009; 193: W202–208. doi: 10.2214/AJR.08.2069.

[18] Mochizuki K, Gabata T, Kozaka K, et al. MDCT findings of extrapancreatic nerve plexus invasion by pancreas head carcinoma: correlation with en bloc pathological specimens and diagnostic accuracy. Eur Radiol 2010; 20: 1757–1767. doi: 10.1007/s00330-010-1727-5.

[19] Sai M, Mori H, Kiyonaga M, Kosen K, Yamada Y, Matsumoto S. Peripancreatic lymphatic invasion by pancreatic carcinoma: evaluation with multi-detector row CT. Abdom Imaging 2010; 35: 154–162. doi: 10.1007/s00261-008-9461-z.

[20] Zhang XM, Mitchell DG, Witkiewicz A, Verma S, Bergin D. Extrapancreatic neural plexus invasion by pancreatic carcinoma: characteristics on magnetic resonance imaging. Abdom Imaging 2009; 34: 634–641. doi: 10.1007/s00261-008-9440-4.

[21] Brennan DD, Zamboni GA, Raptopoulos VD, Kruskal JB. Comprehensive preoperative assessment of pancreatic adenocarcinoma with 64-section volumetric CT. Radiographics 2007; 27: 1653–1666. doi: 10.1148/rg.276075034.

[22] National Comprehensive Cancer Network. Pancreatic adenocarcinoma. NCCN clinical practice guidelines in oncology (NCCN Guidelines)2011.

[23] Tamm EP, Silverman PM, Charnsangavej C, Evans DB. Diagnosis, staging, and surveillance of pancreatic cancer. AJR Am J Roentgenol 2003; 180: 1311–1323. doi: 10.2214/ajr.180.5.1801311.